[CANCER RESEARCH 64, 3380–3385, May 15, 2004]

Advances in Brief

Loss of Tumorigenicity and Metastatic Potential in Carcinoma Cells Expressing the Extracellular Domain of the Type 1 Insulin-Like Growth Factor Receptor

Amir Abbas Samani,[1,3] Eric Chevet,[2,4] Lucia Fallavollita,[2,3] Jacques Galipeau,[5] and Pnina Brodt[1,2,3]

Departments of [1]Medicine and [2]Surgery, McGill University Health Center, [3]Royal Victoria Hospital, [4]Organelle Signaling Laboratory, and [5]the Lady Davis Institute, McGill University, Montreal, Quebec, Canada

Abstract

The receptor for the type 1 insulin-like growth factor (IGF-IR) was identified as a major regulator of the malignant phenotype and a target for cancer therapy. In the present study, a novel IGF-IR mutant consisting of the entire extracellular domain of the receptor (IGFIR^{933}) was genetically engineered and expressed in highly metastatic H-59 murine lung carcinoma cells. We show here that the cells expressed a truncated heterotetramer (β^m-α-α-β^m) that was secreted into the medium and could neutralize the effects of exogenous IGF-I, thus diminishing IGF-I-induced signaling and blocking IGF-I-mediated cellular functions such as cell proliferation, invasion, and survival. *In vivo*, tumor incidence and growth rate were markedly reduced in mice inoculated s.c. with H-59/IGFIR^{933} cells. Moreover, after the intrasplenic/portal inoculation of these cells, there was a 90% reduction in the incidence of hepatic metastases and a significant increase in the long-term, disease-free survival of the mice compared with controls. Our results identify the IGFIR^{933} as a potent antitumorigenic and antimetastatic agent with potential applications for cancer gene therapy.

Introduction

The receptor for the type 1 insulin-like growth factor (IGF-IR) has been implicated in the acquisition of a transformed phenotype and identified as a positive regulator of cell survival and growth in a range of tumor types (1, 2). In many human malignancies, up-regulated expression of IGF-IR, IGF-I, IGF-II, or combinations thereof have been documented. Suppression of IGF-I or IGF-IR expression or function by various strategies led to *in vivo* tumor growth inhibition in various animal models (3, 4), identifying the IGF receptor/ligand system as a target for anticancer therapy.

The IGF-IR is a type 2 tyrosine kinase receptor with a high degree of homology to the insulin receptor. IGF-IR is synthesized as a single-chain prepropeptide with a 30-amino-acid signal peptide that is cleaved after translocation of the nascent chain to the endoplasmic reticulum. After glycosylation and dimerization, the propeptide is processed at a furin cleavage site to yield α and β subunits. These subunits form a β-α-α-β heterotetramer (through disulfide bonds), which is transported to the plasma membrane. Mutations in the transmembrane domain of the receptor (amino acids 936–958) that disrupt membrane anchoring can lead to the production of a soluble, secreted receptor (5).

Previously we reported that cells of the Lewis lung carcinoma subline H-59 overexpress IGF-IR (4×10^3 binding sites/cell) and that their metastatic phenotype is regulated by this receptor (6, 7). Here we describe the effects of transduction of these cells with a retroviral vector encoding a novel, 933-amino-acid soluble peptide spanning the entire extracellular domain of the IGF-IR and show that this peptide is a potent inhibitor of tumor growth and metastasis *in vivo*.

Materials and Methods

Cell Lines. The metastatic H-59 and 293GPG-based packaging cell lines have been described in detail previously (8).

Vector Construction and Transfection. A cDNA fragment corresponding to the first 2844 nucleotides of the human IGF-IR RNA that encode the 933-amino-acid extracellular domain of IGF-IR was amplified by PCR from the full-length cDNA by use of the IGFIR vector (a kind gift from Dr. D. LeRoith, NIH, Bethesda, MD). The amplified fragment, designated IGFIR^{933}, was cloned into the pcDNA4/myc-His vector (Invitrogen) to generate pIGFIR$^{933\text{-His}}$. H-59 cells were transfected with 5 μg of pIGFIR$^{933\text{-His}}$ by use of Lipofectamine (Invitrogen). Transfectants (H-59/IGFIR$^{933\text{-His}}$) were selected by use of 100 μg/ml Zeocin (Invitrogen) and used in this study without further cloning to avoid clonal effects. H-59 cells were also transfected with the pcDNA4/myc-His vector to generate mock-transfected cells. For construction of the retroviral vectors, a cDNA fragment was generated according to the protocol described above, except that a stop codon (*TGA*) was introduced into the antisense primer. The amplified fragment was cloned into the AP-2^{GFP} plasmid downstream of the *cmv* promoter to generate pLTR-IGIR^{933}.

Production of Retroviral Particles and Viral Transduction. The 293GPG packaging cell line was cotransfected with 5 μg of pLTR-IGFIR^{933} and 0.2 μg of the pcDNA3.1-Zeo$^+$ by use of Lipofectamine. Retrovirus production and viral transduction were performed as we described previously (8). Briefly, H-59 cells were transduced with vLTRIGFIR^{933} (or control vector vLTR-GFP) at a multiplicity of infection of 1–2. Highly fluorescent cells (top 30%) were sorted from the transduced population by a fluorescence-activated cell sorter. These cells (H-59/IGFIR^{933}) were used for all of the experiments described.

Western Blot Assay. Tumor cell-conditioned media were filtered and concentrated 80-fold. Proteins were then loaded on a 5.5% polyacrylamide gel and separated by PAGE under nonreducing conditions. Western blotting was performed as we reported previously (8), using the AF-305 antibody (R&D Systems). Proteins were also separated on 7.5 or 15% SDS–polyacrylamide gels under reducing conditions and probed with the anti-IGF-IR antibodies H-60 or C-20 (for proteins separated on 7.5% gels) or with anti-vascular endothelial growth factor (VEGF)-C (H-190) and anti-VEGF (A-20) antibodies (Santa Cruz Biotechnology). For some of the analyses, the concentrated conditioned media derived from H-59/IGFIR$^{933\text{-His}}$ or H-59/His cells were first affinity-purified using nickel-nitrilotriacetic acid (Ni-NTA) metal-affinity chromatography (Qiagen). The mixture was incubated for 2 h at 4°C on an end-over-end shaker and centrifuged for 10 s; the pellet was then washed and processed according to the manufacturer's instructions (QIAexpressionist; Qiagen). Purified proteins were then analyzed by Western blotting with the anti-His antibody (Invitrogen).

Functional *in Vitro* Assays. Cellular proliferation and invasion were measured by the 3-(4,5-dimethylthiazol-2-yl)-2,5-diphenyltetrazolium bromide (MTT) and Matrigel assays, respectively, as we reported previously (8). Cell proliferation was induced by use of recombinant human IGF-I (USBiological, Swampscott, MA) or Des(1–3)IGF-I (GroPep, Thebarton, Australia). The ability of the cells to grow in a 3-dimensional matrix was measured by use of

Received 12/3/03; revised 2/19/04; accepted 3/11/04.

Grant support: Terry Fox Frontiers initiative grant from the National Cancer Institute of Canada (to P. Brodt) and a McGill University Health Center Research Institute award (to A. Samani).

The costs of publication of this article were defrayed in part by the payment of page charges. This article must therefore be hereby marked *advertisement* in accordance with 18 U.S.C. Section 1734 solely to indicate this fact.

Requests for reprints: Pnina Brodt, Division of Surgical Research, McGill University Health Center, Royal Victoria Hospital, Room H6.25, 687 Pine Avenue West, Montreal, Quebec, Canada H3A 1A1. Phone: (514) 842-1231, ext. 36692; Fax: (514) 843-1411; E-mail: pnina.brodt@muhc.mcgill.ca.

Matrigel-coated plates. Cells (5×10^4/well) were seeded in 24-well plates that were precoated with 14 μg/ml Matrigel (Collaborative Research) and cultured in serum-free medium containing 100 ng/ml IGF-I. The medium was replenished on alternate days. Images were captured daily for 10 days with a Nikon microscope equipped with a Northern Eclipse image analysis station (Empix Imaging). Cell density was measured on day 10 by the MTT assay, as described previously (8). The ability of IGF-I to rescue tumor cells from serum-deprivation-induced apoptosis was analyzed by use of fluorescence-labeled Annexin-V. Tumor cells in 35-mm plates (5×10^5/plate) were incubated, first for 24 h in serum-containing medium and then for 48 h in serum-free RPMI medium containing, or not, 10 ng/ml recombinant human IGF-I. Apoptotic cells were detected by the Annexin-V-FLUOS staining kit or Annexin-V-Alexa-586 (Roche), according to the manufacturer's instructions.

IGF-I-Induced Extracellular Signal-Regulated Kinase (ERK) Phosphorylation. Cell signaling in response to IGF-I was analyzed by measuring ERK phosphorylation, as we described previously (9).

To determine whether the soluble receptor could act as a decoy to block IGF-I binding in nonproducer cells, medium conditioned by virally transduced H-59 cells was collected, filtered, and concentrated ~10-fold by use of a 50-kDa-cutoff Centriprep column (Millipore). IGF-I was added to the concentrated medium to a final concentration of 10 ng/ml. The mixture was incubated overnight on ice in an orbital shaker and added to serum-starved H-59 cells for a 20-min incubation at 37°C before analysis of ERK phosphorylation (9). IGF-I-treated (10 ng/ml) cells were used as controls.

***In Vivo* Tumorigenesis and Experimental Metastasis Assays.** Female C57BL/6 mice were administered tumor cells by s.c. injection or by the intrasplenic/portal route, and tumor growth or liver metastases, respectively, were measured, as we described in detail elsewhere (6). For survival studies, the mice were euthanized when they appeared moribund, according to the McGill University animal care guidelines. To harvest tumor cells from the livers, the livers were minced and digested in PBS-EDTA containing 0.05% trypsin. Connective tissue and debris were removed by filtration through a mesh sieve, and the cells were washed and plated in RPMI-FCS. Subcutaneous tumors were surgically removed and processed in a similar manner. Fluorescence-activated cell-sorter (FACS) analysis was performed on the cultured cells 1 week later.

Immunohistochemistry and Terminal Deoxynucleotidyl Transferase (Tdt)-Mediated Nick End Labeling (TUNEL) Assay. Tumor cell apoptosis and proliferation *in vivo* were analyzed by the TUNEL assay and Ki-67 immunostaining, respectively. Mice were inoculated with 10^5 tumor cells by the intrasplenic/portal route and euthanized on day 5; the livers were then perfused via the portal vein with a solution of 4% paraformaldehyde in PBS, excised, fixed in 4% paraformaldehyde for an additional 48 h, and then placed in a solution of 30% sucrose for 4 days before preparation of 7-μm cryostat sections. To detect apoptotic cells, the frozen sections were washed with PBS and incubated with the TUNEL buffer mixture containing the TdT enzyme (Promega) and biotin-labeled dUTP (Roche) for 2 h at 37°C. To visualize TUNEL-positive nuclei, the sections were incubated with Cy3-conjugated streptavidin for 30 min at room temperature. For labeling with anti-Ki-67 antibodies, the sections were first treated with a blocking buffer containing 10% donkey serum and then incubated with a 1:10 dilution of the anti-Ki-67 antibody (Chemicon) and a Cy-2-conjugated donkey antimouse IgG (Jackson Immunoresearch), each for 1 h at room temperature.

Statistics. The two-tailed Student's *t* test was used to analyze data from the functional *in vitro* assays and the metastasis assays. The Kaplan–Meier survival curve and the Log-Rank test were used with Statistica software to analyze the survival data.

Results

Production and Secretion of IGFIR$^{933\text{-}His}$ by H-59 Carcinoma Cells. The cDNA encoding the 933-residue extracellular portion of IGF-IR was initially cloned in the pcDNA4/myc-His plasmid to generate His-tagged molecules that could be used to monitor receptor secretion into the culture medium. Western blot analysis with goat anti-hIGF-IR antibody (AF-305; Fig. 1*C*) revealed that H-59/IGFIR$^{933\text{-}His}$, but not control H-59/His cells, secreted a high-molecular-weight protein that, under nonreducing conditions, migrated in the ≫200-kDa region of the PAGE gel, corresponding to the β^m-α-α-β^m tetramer (Fig. 1*A*; Ref. 5). A protein that migrated in this region was also detected when proteins from the conditioned medium were affinity-purified on nickel beads and the blots were probed with an anti-His antibody (Fig. 1, *A, bottom* and *C*).

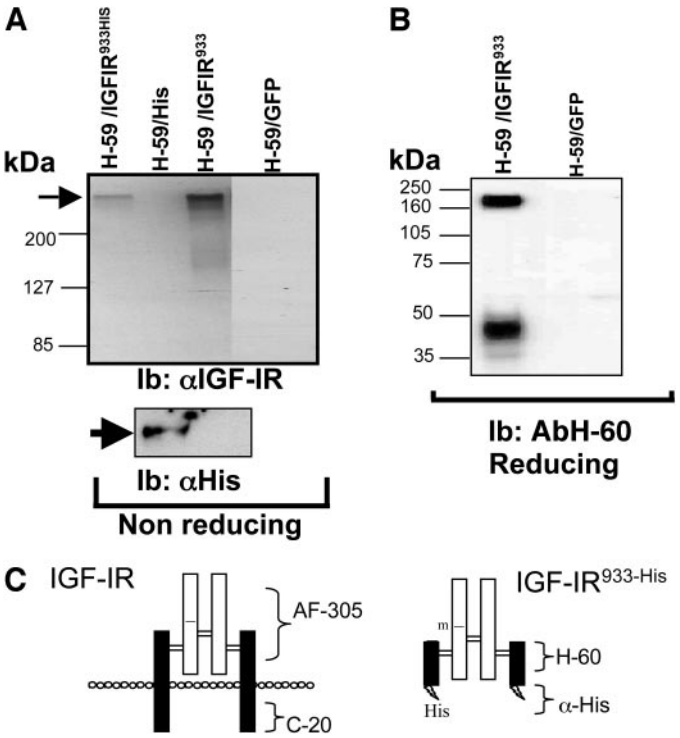

Fig. 1. IGFIR^{933} is secreted into the conditioned medium of producer cells. Western blot analysis was performed on concentrated tumor-conditioned media under nonreducing (*A*) or reducing (*B*) conditions with goat antibody AF-305 to the extracellular domain of the type I insulin-like growth factor receptor (*IGF-IR*; *A, top*) at a dilution of 1:100, a mouse anti-His antibody (*A, bottom*) at a dilution of 1:5000, or the rabbit antibody H-60 to the extracellular portion of the β subunit (*B*) at a dilution of 1:200. Before probing with the anti-His antibody (*A, bottom*), the His-tagged IGFIR^{933} was purified from the conditioned medium by nickel-nitrilotriacetic acid-coated agarose beads. Horseradish peroxidase-conjugated donkey antigoat (*A, top*), antimouse (*A, bottom*), or antirabbit (*B*) IgG antibodies were used as secondary antibodies. *Ib*, immunoblotting; *GFP*, green fluorescent protein. The specificities of the primary antibodies are depicted in the diagrams shown in *C*.

Production and Analysis of vLTR-IGFIR^{933} Retrovirus-Transduced Cells. As a second approach for gene transfer, and in an effort to achieve higher transgene expression and develop a tool for monitoring tumor cells *in vivo*, retroviral particles expressing the truncated receptor in a bicistronic transcript with green fluorescent protein (GFP) were also produced. H-59 cells were transduced with vLTR-IGFIR^{933} VSV/G-pseudotyped retroviruses at a multiplicity of infection of 1 and FACS-sorted to select a subpopulation expressing high GFP levels (top 30%). FACS analysis indicated that the efficiency of gene transfer in these cells (H-59/IGFIR^{933}) was 85% with a mean intensity of fluorescence (MIF) of 20–30. H-59 cells were also transduced with vLTR-GFP retroparticles. Eighty percent of the transduced cells (H-59/GFP) were GFP positive with a MIF of 142.

Similar to H-59/IGFIR$^{933\text{-}His}$ cells, Western blot analysis confirmed that H-59/IGFIR^{933} (but not control) cells expressed and secreted a high-molecular-weight protein that (under nonreducing conditions) migrated in the >200-kDa region of the gel corresponding to the β^m-α-α-β^m tetramer. This protein was specifically recognized by an antibody to the extracellular domain of the receptor (antibody AF-305; Fig. 1*A*). Expression levels in the virally transduced cells were 5-fold higher than in the stably transfected polyclonal H-59/IGFIR$^{933\text{-}His}$ cells (Fig. 1*A*), making these cells a more suitable model for long-term *in vivo* investigations.

In an attempt to further characterize the secreted protein, we subjected tumor-conditioned medium to SDS-PAGE analysis under reducing conditions and immunoprobed the protein blots with two additional antibodies recognizing peptide sequences in the cytoplasmic (antibody C-20) and extracellular (antibody H-60) domains of the IGF-IRβ subunit (Fig. 1*C*). Antibody H-60 detected two bands that migrated at ~202 and 44.5 kDa, corresponding to the calculated molecular mass of the truncated IGF-IR propeptide and the β^m subunit, respectively (Fig. 1*B*). These bands were undetectable in medium conditioned by H-59/GFP cells and were not seen when the blots were probed with antibody C-20, which recognizes the cytoplasmic region of the β subunit (data not shown).

Loss of IGF-IR-Dependent Functions in Cells Producing IGFIR^{933}. We analyzed the effect of IGFIR^{933} production on the ability of the tumor cells to respond to IGF-I, using both H-59/IGFIR$^{933\text{-His}}$ and H-59/IGFIR^{933} cells. Shown in Fig. 2 are the results obtained with H-59/IGFIR$^{933\text{-His}}$ cells. We found that production of a soluble form of IGF-IR inhibited IGF-I-dependent cellular proliferation (Fig. 2*A*). It also reduced IGF-I-mediated cell rescue from serum-deprivation-induced apoptosis and Matrigel invasion by 72 and 65%, respectively, relative to mock-transfected cells (Fig. 2*B*). This suggested that IGFIR$^{933\text{-His}}$ was secreted as a properly folded protein, able to associate with IGF-I and inhibit its biological functions, probably by competing with its binding to endogenous IGF-IR.

IGF-IR-mediated functions were similarly disrupted in H-59/IGFIR^{933} cells. When cell signaling in response to exogenously added IGF-I was analyzed in these cells, we found that ERK phosphorylation in response to IGF-I was markedly reduced (49%) compared with the control, H-59/GFP cells (Fig. 3*A*, *top panel*). Moreover, when IGF-I was preincubated with medium conditioned by H-59/IGFIR^{933} and then added to H-59/GFP cells, ERK phosphorylation was reduced by 57% as compared with cells stimulated with mock-treated IGF-I (Fig. 3*A*, *bottom panel*), suggesting that the secreted receptor was able to bind its ligand and act as a decoy receptor.

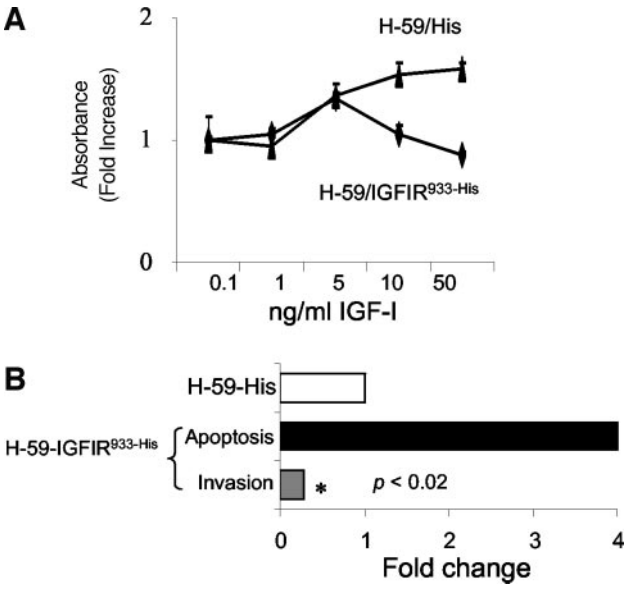

Fig. 2. Reduced type I insulin-like growth factor receptor (IGF-IR) functions in H-59 cells expressing His-IGFIR^{933}. *A*, cell proliferation was measured by the 3-(4,5-dimethylthiazol-2-yl)-2,5-diphenyltetrazolium bromide assay. Shown are the results of a representative experiment of three performed. Results are expressed as means and SD (*bars*) of triplicate samples ($n = 3$; *; $P < 0.02$). *B*, to measure apoptosis, tumor cells were incubated for 48 h in serum-depleted medium containing 10 ng/ml IGF-I. The apoptotic cells were detected with the Annexin-V-FLUOS staining kit after exclusion of propidium iodide-positive cells. Tumor cell invasion in response to IGF-I was measured with the Matrigel invasion assay. Tumor cells were placed on 8-μm Nucleopore filters coated with 0.23 mg/ml Matrigel. IGF-I (10 ng/ml) was added in the lower chamber to induce invasion. Results of these analyzes are expressed as fold change relative to mock-transfected H-59-His cells that were assigned a value of 1 (*, $P < 0.02$).

The attenuation of IGF-I-induced signaling in H-59/IGFIR^{933} cells was reflected by the reduced IGF-I-dependent cellular proliferation as measured in a monolayer (Fig. 3*B*) or a three-dimensional Matrigel model (Fig. 3*C*). IGF-I-mediated cell rescue from serum-deprivation-induced apoptosis, as measured by Annexin-V-Alexa 586 labeling, and cell invasion, as measured by a Matrigel assay, were also reduced in these cells relative to the control cells (67 and 47% reduction, respectively; Fig. 3*D*). Moreover, the expression of VEGF and VEGF-C, two IGF-I-regulated angiogenic factors, was significantly reduced in H-59/IGFIR^{933} (2.5- and 1.7-fold, respectively) as revealed by Western blot analysis (Fig. 3*E*).

IGF-I binding to the receptor is modulated through the activity of the IGF-binding proteins (IGFBP-1 through -6; Ref. 2). Using a ligand binding assay, we previously showed that H-59 cells produce three binding proteins corresponding to IGFBP-1 (or -5), -2, and -3 (10). To investigate whether the binding proteins play a role in mediating the suppressive effect of soluble IGF-IR on IGF-I-mediated cellular responses, we used an IGF-I analog with a mutation in the NH_2-terminal domain, Des(1–3)IGF-I (deletion of residues 1–3) with reduced affinity for IGFBP (11). The ability of the intact and mutated IGFs to induce tumor cell proliferation was analyzed with the MTT assay. As the results in Fig. 3*F* show, the response of H-59/GFP cells to either of these ligands was significantly higher than that elicited in H-59/IGFIR^{933} cells, and H-59/IGFIR^{933} cells responded poorly to both ligands, suggesting that the effect of the soluble receptor was independent of the activity of the IGFBP.

Loss of Tumorigenicity in H-59 Cells Transduced with vLTR-IGFIR^{933}. We next investigated the ability of the virally transduced H-59 cells to form local tumors after the s.c. inoculation of 10^5 cells. All mice receiving injections of H-59/GFP cells developed local tumors by day 7 postinoculation. These tumors grew rapidly, reaching a mean volume of 2838 mm^3 and causing morbidity by day 18. In contrast, only 50% of the mice inoculated with H-59/IGFIR^{933} cells developed tumors, and these tumors grew at a significantly reduced rate relative to controls ($P < 0.0005$ from day 7 onward), reaching a mean tumor volume of only 234 mm^3 by day 18 (Fig. 4*A*). The remaining 50% of the mice did not develop tumors for 6 months, at which time the experiment was terminated.

Expression of IGFIR^{933} also suppressed the ability of the tumor cells to form hepatic metastases after intrasplenic/portal inoculation. Results of two separate experiments are shown in Fig. 4*B*. All mice receiving injections of H-59/GFP cells developed multiple liver metastases by day 14 postinjection, and the numbers of metastases/liver in these mice ranged from 38 to >200 (median, 200). In contrast, only 12% of those receiving injections of H-59/IGFIR^{933} cells developed detectable metastases at this time, and the number of metastases/liver in these mice did not exceed 2. This marked reduction in metastatic ability was reflected in a significant extension to animal survival, as shown in Fig. 4*C*. Whereas all mice receiving injections of H-59/GFP cells were moribund with multiple liver metastases by days 19–21 after tumor cell inoculation, no morbidity was apparent in any of the mice receiving H-59/IGFIR^{933} cells until day 34. Additional mice (50% in total) were moribund by day 41 ($P < 0.0002$). Interestingly, in these mice the cause of morbidity was not hepatic metastases (which were undetectable), but the growth of intra-abdominal, extrahepatic tumor masses in proximity to the injection site (data not shown). The remaining mice in this group (50%) remained tumor free for 6 more months, at which time the experiment was terminated.

To investigate the role of apoptosis in this process, we performed an additional experiment in which we excised the livers 5 days after tumor cell injection, prepared cryostat sections, and analyzed the

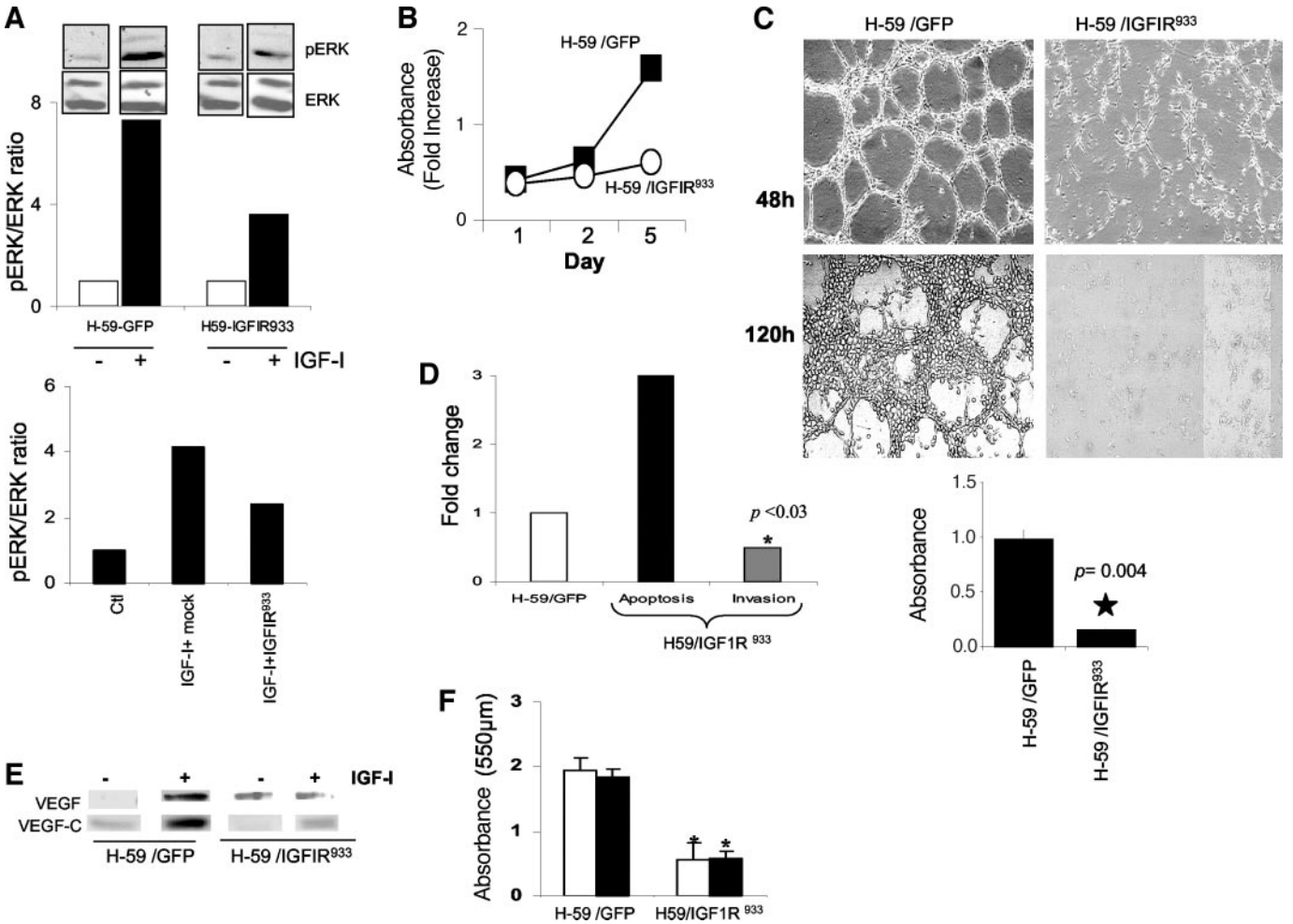

Fig. 3. Loss of insulin-like growth factor-I (*IGF-I*) responsiveness in virally transduced, IGFIR^{933}-expressing cells. *A*, *top*, extracellular signal-regulated kinase phosphorylation (*pERK*/*ERK*) was measured after incubation of tumor cells with 10 ng/ml IGF-I for 20 min. Cell lysate proteins were separated on 10% SDS-polyacrylamide gels, and the transferred proteins were probed successively with antibodies to Phospho-p44/42 mitogen-activated protein kinase, p44/42 mitogen-activated protein kinase, and tubulin. Shown are the results of a representative experiment of two performed. *Bottom*, IGF-I (at a final concentration of 10 ng/ml) was preincubated overnight with concentrated H-59/IGFIR^{933} or H-59/green fluorescent protein (GFP)-conditioned media and then added to H-59 cells for 20 min before cell lysis. Western blots were performed as described above. *Ctl*, control. *B*, serum-starved tumor cells grown in monolayer cultures were incubated with 10 ng/ml IGF-I, and cell proliferation was quantified on the indicated days by the 3-(4,5-dimethylthiazol-2-yl)-2,5-diphenyltetrazolium bromide (MTT) assay. *C*, growth of the cells in a three-dimensional matrix was evaluated by use of Matrigel-coated wells containing IGF-I. Cell growth was monitored by light microscopy. Shown are representative microscopic fields as seen on days 2 and 5 (magnification, ×30). To quantify the number of cells growing in Matrigel (*bar graph*), MTT was added to the plates on day 10, and the absorbance was measured at 550 and 630 nm. *D*, IGF-I-dependent rescue from apoptosis (■), analyzed with the Annexin-V-Alexa 586 kit, and the invasion assay (▨) were performed as described in the legend to Fig. 2. Results are expressed as fold change relative to mock-transduced H-59/GFP cells (□), which were assigned a value of 1 ($n = 2$; ∗, $P < 0.03$). *E*, Western blotting was performed on concentrated condition media after the cells were incubated (or not) with 10 ng/ml IGF-I for 48 h. *VEGF*, vascular endothelial growth factor. *F*, serum-deprived tumor cells were incubated with 10 ng/ml IGF-I (□) or Des(1–3)IGF-I (■) for 48 h, and cell viability was quantified by the MTT assay (∗, $P < 0.002$ compared with control H-59/GFP cells).

sections by TUNEL assay and Ki-67 staining. We found that although control cells formed small hepatic colonies by day 5 that consisted mainly of Ki-67^{+} and TUNEL^{-} cells, the H-59/IGFIR^{933} cells could be detected only as intrasinusoidal single cells that were Ki-67^{-} and TUNEL^{+}(Fig. 4*D*), suggesting that the lack of IGF-I responsiveness induced apoptosis in the early stages of liver colonization.

To investigate whether the growth of H-59/IGFIR^{933} tumors *in vivo* resulted from the selection of a subpopulation of cells with reduced transgene expression, we harvested tumor cells from the s.c. and hepatic tumors and expanded them *in vitro*. Their GFP expression levels as measured by FACS were then compared with the expression levels in the initial stock of cells that were used for the injections, as means of assessing changes in transcript levels. This analysis revealed reductions of 40% in the proportion of GFP^{+} cells and 80% in MIF values for cells derived from the hepatic tumors, whereas MIF values for cells isolated from the s.c. tumors were reduced by 30%. In contrast, the incidence and MIF values for the control, H-59/GFP cells retrieved from either of the sites remained unchanged (Fig. 4*E*).

Discussion

The objective of this study was to generate a recombinant, soluble IGF-IR protein that could function as a decoy receptor and ultimately be used to inhibit tumor growth *in vivo*. We show here that a protein corresponding to the complete extracellular portion of the receptor was able to neutralize the effects of exogenous IGF-I—a process independent of the activities of the IGFBPs—and that its secretion had a potent growth-inhibitory effect on the producing cells both *in vitro* and *in vivo*. Indeed, *in vivo*, the expression of this protein blocked tumor growth in several anatomical sites, including the liver, identifying IGFIR^{933} as a potential anticancer therapeutic agent. The data suggest that this effect was mediated by the induction of tumor apoptosis *in vivo* early after the injection of the cells.

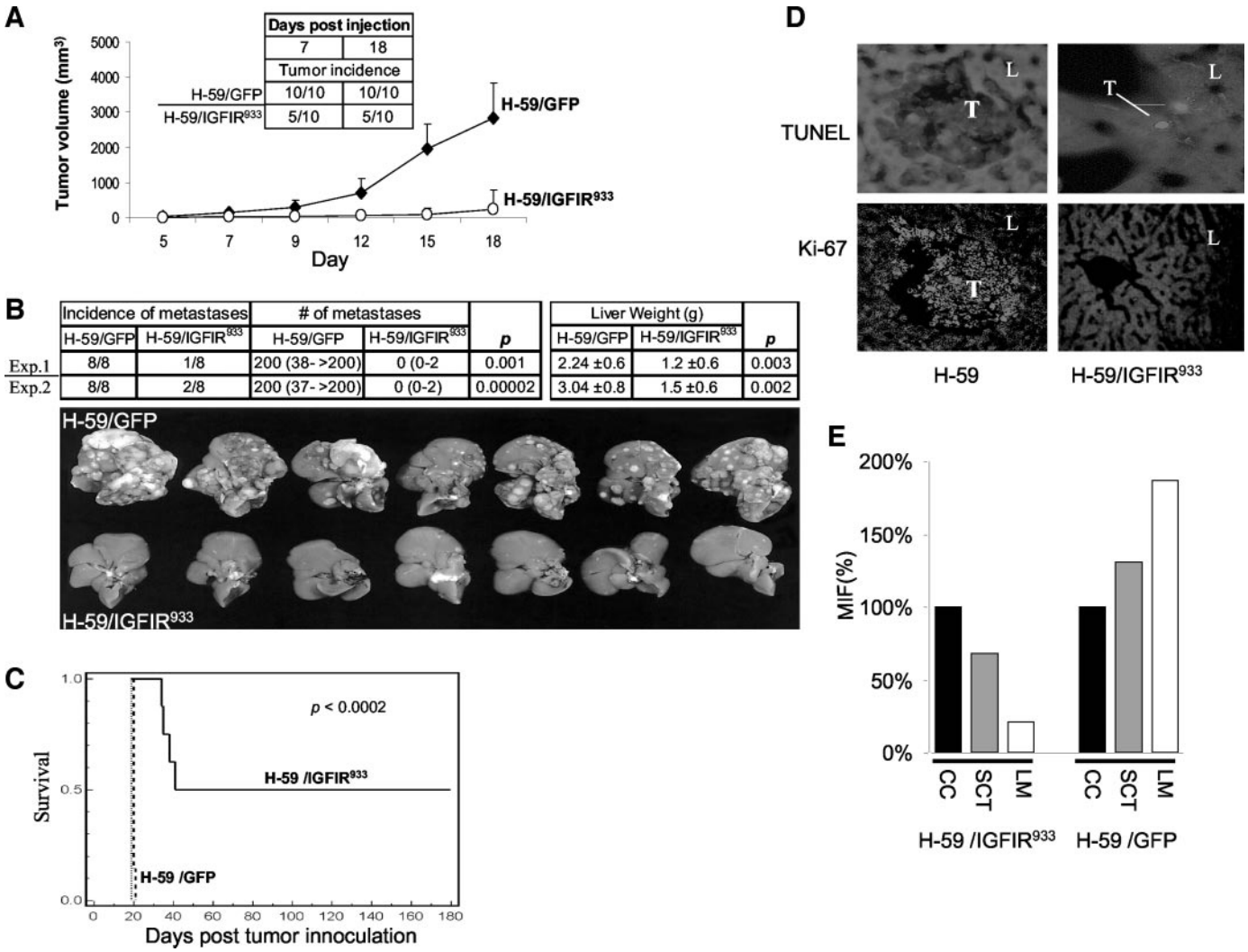

Fig. 4. Loss of tumorigenicity and metastatic potential of H-59/IGFIR^{933} cells. *A*, mice received s.c. injections of 2×10^5 tumor cells, and tumors were measured on alternate days. Shown are the results of a representative experiment of three performed in which 7–10 mice were inoculated per group. *GFP*, green fluorescent protein. *B*, liver metastases were enumerated 14 days after the intrasplenic/portal injection of 10^5 tumor cells. Results (*top*) are expressed as the median (range) of metastases/liver based on eight animals per group. Liver weights (means ± SD) are shown on the *right*, and representative livers from experiment (*Exp.*) 2 are shown on the *bottom*. Shown in *C* are survival data for mice inoculated with tumor cells by the intrasplenic/portal route to generate experimental hepatic metastases ($n = 2$; $P < 0.0002$). *D*, terminal deoxynucleotidyl transferase (Tdt)-mediated nick end labeling (*TUNEL*) assay (*top*) and Ki-67 staining (*bottom*) were performed on liver (*L*) cryostat sections prepared 5 days post-tumor (*T*) injection (magnification, ×135). *E*, tumor cells were harvested from liver metastases (*LM*) or s.c. tumors (*SCT*) and analyzed by flow cytometry. Shown are mean intensity of fluorescence (*MIF*) values relative to the cultured cells (*CC*) that were originally used for the injections.

In media conditioned by tumor cells that were either transfected with the IGFIR^{933}-expressing plasmid or transduced with vLTR-IGFIR^{933} particles, a protein corresponding to the β^m-α-α-β^m heterotetramer (5) was detected under nonreducing conditions by Western blotting. This suggests that the truncated propeptide was correctly processed post-translationally in the secretory pathway and assembled into a truncated tetramer. IGF-IR maturation requires glycosylation, proteolytic cleavage, and homo-/heterodimerization by disulfide linkage during the transport from the endoplasmic reticulum to the Golgi and then to the cell surface. The presence of the truncated tetramer in the medium and the ability of the soluble receptors to bind IGF-I suggest that the truncated propeptide was processed to generate a correctly folded recombinant receptor. This is consistent with an earlier study by Jansson *et al.* (5) that showed propeptide processing, receptor assembly, and ligand binding of a fusion protein consisting of the first 932 amino acids of the IGF-IR peptide and an IgG-binding protein domain. When Western blotting was performed under reducing conditions, a 44.5-kDa protein corresponding to β^m was detected in the conditioned media; in addition, a second, 202-kDa protein corresponding to the truncated IGF-IR proreceptor with an intact cleavage site was also revealed by domain-specific antibodies. The secretion of this molecule by the transduced cells was unexpected, and the underlying mechanism is unclear. It may indicate that overproduction of the recombinant receptor in these cells caused a saturation of the endoplasmic reticulum processing pathway (12), leading to the release of partially processed molecules. Interestingly, it was recently shown that the expression of a deletion mutant of IGF-IR lacking the 36 amino acid residues immediately NH_2-terminal to the transmembrane domain of IGF-IR (IGF-IR$^{\Delta 870-905}$) in BALB/c 3T3 cells resulted in the intracellular accumulation of a high-molecular-mass (~200 kDa) proreceptor (13). Another study showed that the insulin proreceptor can bind insulin (14); it is therefore possible that the structurally similar IGF-IR proreceptors can also retain a ligand-binding capacity.

In the present study, a polyclonal population of transduced cells was used for the experiments. We chose this approach because it mimics more closely the effects that viral transduction may have on tumors growing *in vivo*. The heterogeneity in transgene expression in

these cells could explain the appearance of liver metastases (12%) and s.c. tumors (50%) in some of the inoculated mice. FACS analysis performed on tumor cells that were recovered from these sites showed that, in fact, their GFP expression was significantly reduced relative to the original tumor cell population, suggesting that they may have been selected *in vivo* for low transgene expression levels. This could also explain the eventual appearance of intra-abdominal tumor masses in some of the mice after intrasplenic/portal inoculation.

Other soluble receptors have been successfully used to block tumor cells growth. Among them are soluble forms of the VEGF receptor flk1 (15), soluble type II and type III transforming growth factor-β receptors (16, 17) and soluble fibroblast growth factor receptor-1 (18). A soluble form of VEGF (VEGF-Trap) has in fact advanced into clinical trials with promising early results (19). The production of a truncated 486-residue peptide corresponding to approximately two thirds of the IGF-IR α subunit has also been reported (20). However, because this truncated receptor cannot form dimers and may not bind ligand extracellularly (21, 22), its mechanism of action appears to be different from that of the 933-residue protein that we describe here. Rather than act as a secretable decoy, the 486-stop receptor may remain associated with the cell and exert its antitumorigenic effect through interaction with endogenous receptors (23).

In previous studies we used an antisense-based approach to suppress IGF-IR expression in H-59 cells (8). This approach led to marked reduction in the incidence of hepatic metastases but had a more limited effect on s.c. tumor growth (8). In the present study, the use of tumor cells expressing a soluble form of the receptor resulted in a significantly higher long-term survival after s.c. or intrasplenic/portal inoculation of the tumor cells (50% survival at 6 months compared with 0% in previous studies). Although it is possible that differences in transgene expression levels in the genetically altered cells used in the two studies may have contributed to the increased efficacy of the soluble receptor strategy, a fundamental difference in the two approaches may also be at play; *i.e.*, while the effect of antisense IGF-IR expression may be limited to the transgene-expressing cells, the production of a secretable receptor could also affect the tumor microenvironment and may impact on the stromal cell response and on tumor-induced angiogenesis, thereby enhancing the tumor-inhibitory effect. Indeed, IGF-I and IGF-II were shown to induce angiogenesis by stimulating endothelial cell migration, differentiation, and survival (24). Their role in tumor-induced stromal reactivity has also been documented (25, 26). Noteworthy in this respect is a recent study by De Meyts and Whittaker (27) demonstrating a loss of negative cooperativity for a soluble insulin receptor. It is possible that a soluble IGF-IR receptor can also bind more than one ligand and that this could contribute to its efficacy as a decoy receptor.

Our results suggest that the soluble IGFIR^{933} molecule could exert its effect on neighboring, nonproducer cells, probably by binding and neutralizing free IGF-I. This property can potentially be exploited by the delivery of high levels of the protein into the tumor or organ sites of metastases by vehicles such as adenoviruses that can be produced at high titers and can transduce both dividing and nondividing cells in the target organ. Adenoviruses have been used successfully to express other soluble receptors, including the fms-like tyrosine kinase receptor sFLT-1, recently used for gene therapy of ovarian cancer (28). Taken together, our results suggest that the soluble IGFIR^{933} peptide could provide a potent tumor-inhibitory molecule with potential applications for therapy of malignant diseases with a known growth dependency on IGF-IR.

Acknowledgments

We are indebted to Dr. D. LeRoith (NIH) for a gift of IGFIR plasmid, to Dr. N. V. Christou (Department of Surgery, McGill University Health Center) for the use of the flow cytometer, and to B. Giannias and J. Sanchez-Darden (FACS facility, McGill University) for their help with the FACS analysis and sorting.

References

1. Brodt P, Samani A, Navab R. Inhibition of the type I insulin-like growth factor receptor expression and signaling: novel strategies for antimetastatic therapy. Biochem Pharmacol 2000;60:1101–7.
2. Samani AA, Brodt P. The receptor for the type I insulin-like growth factor and its ligands regulate multiple cellular functions that impact on metastasis. Surg Oncol Clin N Am 2001;10:289–312.
3. Baserga R. Controlling IGF-receptor function: a possible strategy for tumor therapy. Trends Biotechnol 1996;14:150–2.
4. Surmacz E. Growth factor receptors as therapeutic targets: strategies to inhibit the insulin-like growth factor I receptor. Oncogene 2003;22:6589–97.
5. Jansson M, Hallen D, Koho H, et al. Characterization of ligand binding of a soluble human insulin-like growth factor I receptor variant suggests a ligand-induced conformational change. J Biol Chem 1997;272:8189–97.
6. Long L, Rubin R, Baserga R, Brodt P. Loss of the metastatic phenotype in murine carcinoma cells expressing an antisense RNA to the insulin-like growth factor receptor. Cancer Res 1995;55:1006–9.
7. Brodt P, Fallavollita L, Khatib AM, Samani AA, Zhang D. Cooperative regulation of the invasive and metastatic phenotypes by different domains of the type I insulin-like growth factor receptor beta subunit. J Biol Chem 2001;276:33608–15.
8. Samani AA, Fallavollita L, Jaalouk DE, Galipeau J, Brodt P. Inhibition of carcinoma cell growth and metastasis by a vesicular stomatitis virus G-pseudotyped retrovector expressing type I insulin-like growth factor receptor antisense. Hum Gene Ther 2001;12:1969–77.
9. Zhang D, Brodt P. Type 1 insulin-like growth factor regulates MT1-MMP synthesis and tumor invasion via PI 3-kinase/Akt signaling. Oncogene 2003;22:974–82.
10. Long L, Nip J, Brodt P. Paracrine growth stimulation by hepatocyte-derived insulin-like growth factor-1: a regulatory mechanism for carcinoma cells metastatic to the liver. Cancer Res 1994;54:3732–7.
11. Tomas FM, Knowles SE, Owens PC, et al. Effects of full-length and truncated insulin-like growth factor-I on nitrogen balance and muscle protein metabolism in nitrogen-restricted rats. J Endocrinol 1991;128:97–105.
12. Bass J, Chiu G, Argon Y, Steiner DF. Folding of insulin receptor monomers is facilitated by the molecular chaperones calnexin and calreticulin and impaired by rapid dimerization. J Cell Biol 1998;141:637–46.
13. Li S, Zhang H, Hoff H, Sell C. Activation of the insulin-like growth factor type 1 receptor by deletion of amino acids 870–905. Exp Cell Res 1998;243:326–33.
14. Sasaoka T, Shigeta Y, Takata Y, Sugibayashi M, Hisatomi A, Kobayashi M. Binding specificity and intramolecular signal transmission of uncleaved insulin proreceptor in transformed lymphocytes from a patient with extreme insulin resistance. Diabetologia 1989;32:371–7.
15. Becker CM, Farnebo FA, Iordanescu I, et al. Gene therapy of prostate cancer with the soluble vascular endothelial growth factor receptor flk1. Cancer Biol Ther 2002;1:548–53.
16. Rowland-Goldsmith MA, Maruyama H, Kusama T, Ralli S, Korc M. Soluble type II transforming growth factor-beta (TGF-beta) receptor inhibits TGF-beta signaling in COLO-357 pancreatic cancer cells in vitro and attenuates tumor formation. Clin Cancer Res 2001;7:2931–40.
17. Bandyopadhyay A, Zhu Y, Malik SN, et al. Extracellular domain of TGFbeta type III receptor inhibits angiogenesis and tumor growth in human cancer cells. Oncogene 2002;21:3541–51.
18. Ogawa T, Takayama K, Takakura N, Kitano S, Ueno H. Anti-tumor angiogenesis therapy using soluble receptors: enhanced inhibition of tumor growth when soluble fibroblast growth factor receptor-1 is used with soluble vascular endothelial growth factor receptor. Cancer Gene Ther 2002;9:633–40.
19. J. Dupont DC, Gordon MS, Mendelson D, et al. Phase 1 study of VEGF Trap in patients with solid tumors and lymphoma. Proc Am Soc Clin Oncol 2003;22:194.
20. D'Ambrosio C, Ferber A, Resnicoff M, Baserga R. A soluble insulin-like growth factor I receptor that induces apoptosis of tumor cells in vivo and inhibits tumorigenesis. Cancer Res 1996;56:4013–20.
21. Garrett TP, McKern NM, Lou M, et al. Crystal structure of the first three domains of the type-1 insulin-like growth factor receptor. Nature (Lond) 1998;394:395–9.
22. McKern NM, Lou M, Frenkel MJ, et al. Crystallization of the first three domains of the human insulin-like growth factor-1 receptor. Protein Sci 1997;6:2663–6.
23. Reiss K, Tu X, Romano G, Peruzzi F, Wang JY, Baserga R. Intracellular association of a mutant insulin-like growth factor receptor with endogenous receptors. Clin Cancer Res 2001;7:2134–44.
24. Grulich-Henn J, Ritter J, Mesewinkel S, Heinrich U, Bettendorf M, Preissner KT. Transport of insulin-like growth factor-I across endothelial cell monolayers and its binding to the subendothelial matrix. Exp Clin Endocrinol Diabetes 2002;110:67–73.
25. LeBedis C, Chen K, Fallavollita L, Boutros T, Brodt P. Peripheral lymph node stromal cells can promote growth and tumorigenicity of breast carcinoma cells through the release of IGF-I and EGF. Int J Cancer 2002;100:2–8.
26. Rasmussen AA, Cullen KJ. Paracrine/autocrine regulation of breast cancer by the insulin-like growth factors. Breast Cancer Res Treat 1998;47:219–33.
27. De Meyts P, Whittaker J. Structural biology of insulin and IGF1 receptors: implications for drug design. Nat Rev Drug Discov 2002;1:769–83.
28. Mahasreshti PJ, Navarro JG, Kataram M, et al. Adenovirus-mediated soluble FLT-1 gene therapy for ovarian carcinoma. Clin Cancer Res 2001;7:2057–66.

Loss of Tumorigenicity and Metastatic Potential in Carcinoma Cells Expressing the Extracellular Domain of the Type 1 Insulin-Like Growth Factor Receptor

Amir Abbas Samani, Eric Chevet, Lucia Fallavollita, et al.

Cancer Res 2004;64:3380-3385.